Integrated GPR attribute analysis for improved thermal structure characterisation of polythermal glaciers

P. Gutgesell and E. Forte

Department of Mathematics, Informatics and Geosciences, University of Trieste, Trieste, Italy

ABSTRACT   This paper reanalyses and reinterprets the GPR data set collected in 2018 on the Von Postbreen polythermal glacier, in the Tempelfjorden region of the Svalbard Islands. Different Ground Penetrating Radar (GPR) attributes were exploited as tools for the detection of peculiar patterns and inapparent glaciological facies in typical reflection amplitude data. Spectral attributes such as dominant frequency, instantaneous phase and sweetness were specifically calculated. In addition, some texture attributes like chaos and entropy were integrated with the previous ones, so as to enable the detection of a peculiar anomalous zone (AZ). This zone is non-ubiquitous, concentrated in specific areas of the glacier, where the ice is thicker and close to the main bedrock topographic highs. By means of thermal models available in the international literature, this AZ was related to local temperature variations, which are the consequence of increased heat transfer mechanisms due to peculiar stress conditions. The proposed approach can be applied to other glaciological GPR surveys on polythermal glaciers in order to obtain improved and more constrained data interpretation and thermal facies imaging.

Key words: Ground Penetrating Radar, polythermal glaciers, GPR attributes, thermal facies, GPR interpretation.

1. Introduction

Detailed data on the internal structure, volume, and distribution of temperate ice in polythermal glaciers is essential to understanding glacial thermal regime, dynamics, and response to climate change (Lamsters *et al*., 2020). Ground Penetrating Radar (GPR) widely demonstrated its effectiveness as a means for measuring glacier thickness and internal structure thanks to the resolution and high penetration of electro-magnetic (EM) signals within ice and frozen materials. In addition, GPR has been exploited to infer glacier thermal structures by extracting information from internal scattering, which is often related to the localised concentration of free water (Pettersson *et al*., 2003; Reinardy *et al*., 2019).

In this study, the GPR data set, discussed by Delf *et al*. (2022) and highlighting the thermal structure of the Von Postbreen polythermal glacier (Svalbard Islands), was reanalysed. Delf *et al*. (2022) used GPR data and focused on diffraction hyperbola analysis as a tool to estimate the velocity of EM waves and, in turn, the amount of water inside the glacier. This analysis aims to further extend the previously obtained results by considering the data signature and distinguishing between different thermal zones inside the glacier through the calculation of various signal attributes. In particular, specific and previously inapparent patterns were found

by not only considering the reflection amplitudes but also other integrated GPR attributes. This approach has proven effective in different glaciological applications, from the detection of warm and cold ice zones to internal glacier mapping (Santin *et al*., 2019; Forte *et al*., 2021), from glaciological transformations and firnification processes (Zhao *et al*., 2016a) to the imaging of buried objects and debris-rich zones within glaciers (King *et al*., 2008; Forte *et al*., 2021). Indeed, one of the main open issues in glaciology is how GPR, often integrated with other measurements (e.g. borehole temperature or geomorphological evidences), can be used to highlight and distinguish the warm/cold ice facies from other zones, which are possibly related to different glaciological processes or features that can occur inside glaciers. All these zones are visualised in amplitude GPR sections as high scattered EM patterns and are usually associated with warm ice or water pockets/channels in the available literature (Pettersson *et al*., 2003; Irvine-Fynn *et al*., 2006; Bælum and Benn, 2011; Seveste *et al*., 2015).

However, the actual physical meaning of the highly diffuse scattering detected by GPR within glaciers is not always obvious. Typically, in polythermal glaciers there is a clear transition from cold to warm ice characterised by different free water contents (e.g. Bælum and Benn, 2011), which are in turn related to different thermal regimes (e.g. Pettersson *et al*., 2003). In GPR glaciological surveys, this type of contact is typically imaged as a transition between an upper layer, with only few reflectors and diffractions, and a less transparent zone, with diffuse scattering (King *et al*., 2008; Reinardy *et al*., 2019). However, in other cases, diffuse scattering is, instead, interpreted as deposits of mixed debris and ice (King *et al*., 2008; Colucci *et al*., 2015).

The same GPR data set, collected in 2018 and published in Delf *et al*. (2022), that images the central portion of the Von Postbreen glacier (Fig. 1), was reanalysed in this paper. The focus was not on data inversion or on the performance of specific processing algorithms but rather on improved data interpretation, exploitation of different GPR attributes so as to specifically analyse frequency and phase data behaviour, through the use of attributes as a tool for detecting peculiar patterns and glaciological facies, which are inapparent in typical reflection amplitude data. In addition, a new thermal interpretation of the glacier, based on improved GPR data analysis and a number of thermal models available in the international literature, were provided.

2. Methods

The GPR data set was collected on the Von Postbreen polythermal glacier (78° 25' N, 17° 42' E) in March 2018 with a PulseEkko Pro GPR instrument (Sensors & Software) equipped with 25 MHz antennas mounted on a plastic staff towed behind a snowmobile. Further details on the data set are reported in the above-mentioned paper. The glacier, located in the Tempelfjorden region of the Svalbard Islands, is approximately 15 km long, with an area of about 168 km^2 (Seveste *et al*., 2015). The GPR survey encompasses a longitudinal profile (maximum and minimum elevations of 668 m and 155 m, respectively) and 11 transversal profiles (Fig. 1) with a total length equal to about 40 km.

The analysis carried out focuses on integrated signal attributes and evaluates their values in the different portions of the glacier. GPR attributes are very similar to the well-known seismic attributes, which are routinely applied to reflection seismic data to extract additional, and more constrained, information from the subsurface, thereby improving data interpretation (Chopra and Marfurt, 2007). A comprehensive review of the application of GPR attributes in glaciological studies is beyond the scope of this paper, and, as far as both instantaneous and texture attributes are concerned, can be found (along with the mathematical background) in Zhao *et al*. (2012, 2016a, 2016b, 2018).

For both GPR data interpretation and signal attribute calculation, the Petrel software platform (v. 2022.1), originally developed for reflection seismic data interpretation but equally suitable for GPR data, was utilised.

GPR data sets usually comprise only 2D profiles, thus preventing the application of several attributes, which use volumetric subsurface imaging and are very common in reflection seismics,
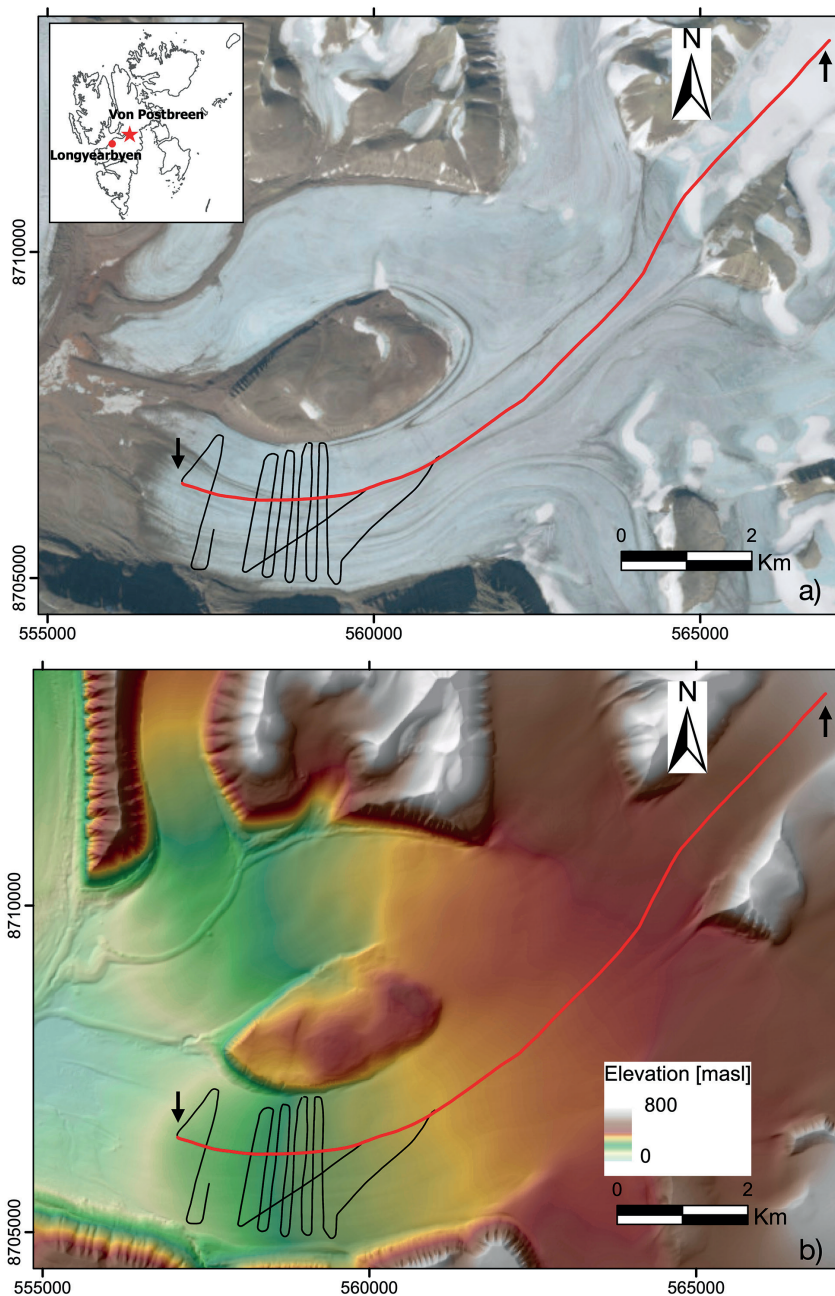

Fig. 1 - Location map of the GPR survey on the Von Postbreen polythermal glacier (Svalbard Islands) superimposed on satellite imagery (a) and on the digital terrain model (b), both taken from the Norwegian Polar Institute Map Data (https://geodata.npolar.no/).

especially for oil and gas exploration and exploitation (Randen and Sønneland, 2005). However, one can find examples of the application of signal attributes on GPR 3D data sets (e.g. Böniger and Tronicke, 2010; Zhao *et al.*, 2012) even if, to the best of our knowledge, this has yet to be carried out for glaciological applications.

Amplitude-related attributes are the most exploited attributes in glaciology, as they can help to detect variations in glacial and frozen materials, emphasising the most relevant reflectors (Zhao *et al.*, 2016a). Instantaneous amplitude (often referred to as reflection strength or trace envelope), along with its deriving attributes (among which, its first derivate, root-mean-square amplitude and different types of energy attributes) belongs to the category of amplitude-related attributes.

Coherency attributes, which measure the similarity or difference between adjacent traces, with even very sophisticated algorithms, are used for similar purposes (e.g. Böniger and Tronicke, 2010), namely for improving the interpretation of features such as, for instance, the glacier ice bottom or internal layering, and main internal discontinuities typically caused by crevasses or glacial moulins.

The continuity/discontinuity of reflectors can be further highlighted by phase-related attributes such as the instantaneous phase or its cosine (Forte *et al.*, 2012), both independent of signal amplitude.

However, important glaciological facies, and, primarily, cold and warm ice, often produce neither high amplitude (or characteristic patterns) nor peculiar phase variations. For this reason, two other attribute categories, namely frequency-related and texture attributes, were accounted for.

At first, various spectral (instantaneous frequency, phase, bandwidth, dominant and mean frequency, sweetness, cosine of instantaneous phase, frequency slope fall) and texture (chaos, entropy, homogeneity) attributes were calculated. The focus was, then, narrowed to three specific spectral attributes, the dominant frequency, the instantaneous phase, and sweetness, and to two specific texture attributes, chaos and entropy.

All data acquisition and processing details are reported in Delf *et al.* (2022), where the processed GPR data set (analysed again in this paper) was made freely available. We decided not to reprocess the data set in order to achieve results that were directly comparable with the results reported in the above-mentioned paper.

2.1. Frequency-related attributes

GPR (as well as seismic) signals typically show a general decrease in high frequency content as recording time increases. This is due to the low-pass filtering effect of geologic materials, especially when characterised by high overall electrical conductivity. Nevertheless, this general trend can, at least partially, be modified when in the presence of local conductivity variations. As a consequence, if local frequency variations can be evaluated as a function of their time and location, then, important information about the changes in the electrical properties of the investigated materials (Forte *et al.*, 2012) can be extracted. This is particularly true for glaciological surveys in which the main spectral shifting effect is usually related to the physical change of state from ice to water, rather than to the ice composition or the presence of specific chemical compounds. Moreover, frozen materials are typically characterised by low overall electrical conductivity, making the use of GPR very favourable.

Frequency-related attributes are calculated with the short-time Fourier transform or with different wavelet analyses. Another slightly different approach is referred to as 'spectral

decomposition' in reflection seismics, and has occasionally been adopted for specific GPR applications (Geerdes and Young, 2007; Böniger and Tronicke, 2012). However, while spectral decomposition is very powerful in seismic data analysis, its applicability to GPR data is less attractive and limited to some peculiar data sets, typically imaging stratigraphic features.

Instantaneous frequency is arguably the most common frequency attribute. Calculated as the derivative of the instantaneous phase for each time sample, it provides information about the spectral variations in time and space. Other similar attributes include dominant frequency (i.e. the frequency with the highest amplitude within a considered time window), median frequency (i.e. the weighted median value of the frequency spectrum above a threshold calculated within a time window), average frequency (i.e. the arithmetic mean of the frequency spectrum), and frequency slope fall (i.e. the peakedness of the spectrum) among others [see e.g. Forte *et al*. (2012) for further details].

In addition, many composite attributes combining frequency and amplitude signal characteristics can be observed. One of the most popular is the sweetness attribute (i.e. the ratio between instantaneous amplitude and instantaneous frequency square root).

2.2. Texture attributes

Texture (or textural) attributes determine the statistical relationship between data within 2D or 3D analysis windows centred on each individual sample. Texture attributes attempt to quantify different mutually related elements in terms of their shape, continuity and pattern, i.e. the signal texture. This technique is well-established in both image and seismic data analysis (Chopra and Alexeev, 2006), and was also successfully tested on GPR data sets (McClymont *et al*., 2008; Zhao *et al*., 2016b).

Haralick *et al*. (1973) proposed 14 different attributes derivable from the texture analysis of seismic data, among which most common are chaos, contrast, entropy, and homogeneity. A comprehensive review of texture attributes applied in geophysics can be found in Gao (2011).

3. Results

The first phase consisted in comparing the GPR amplitude profile reported in Delf *et al*. (2022) (Fig. 2a) with the reinterpreted data (Fig. 2b) of this research. The comparison highlighted some minor differences in the interpretation of the bedrock and in the limit between cold and warm ice, as well as a basal layer of glacial sediment (the dotted cyan line in Fig. 2b), previously not detected. GPR data interpretation was compared with the EM wave velocity field (Fig. 2c) extracted in Delf *et al*. (2022) through a dedicated diffraction focusing analysis, and with the estimated water content (Fig. 2d) obtained from the interval velocities by applying a relation originally proposed by Bradford *et al*. (2009). The Cold/temperate-ice Transition Zone (CTZ) is well imaged by the reflection amplitude (Figs. 2a and 2b) but does not precisely correspond to a velocity field variation or to a water content transition.

In particular, from the interval velocity field inferred by Delf *et al*. (2022), while a high velocity typical of cold ice with negligible water content is imaged in the shallowest 60-100 m of the glacier, for depths higher above the CTZ, velocities show high lateral changes with values ranging from about 0.13 to values close to 0.17 m/ns (Fig. 2c).

Thanks to the integrated signal attributes (Figs. 3, 4, and 5), an anomalous zone (AZ) just above the CTZ boundary in the cold ice region, not visible in the amplitude GPR section, was
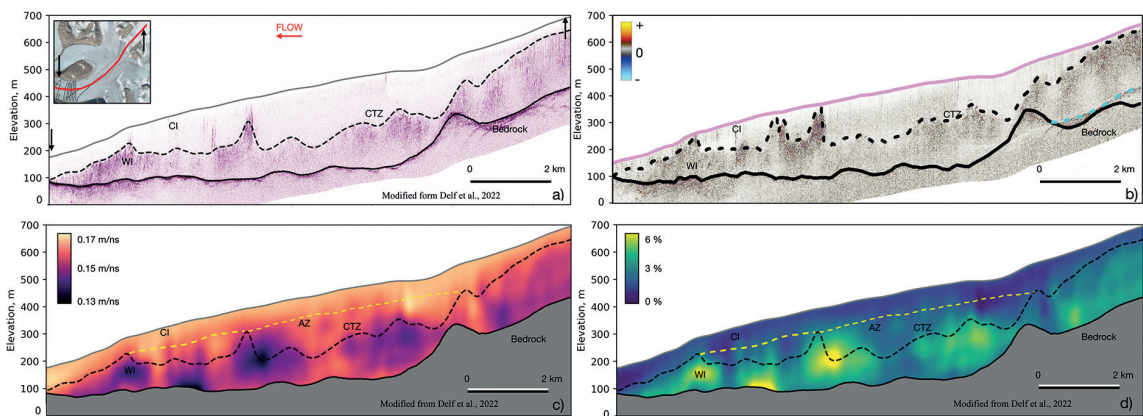
Fig. 2 - GPR longitudinal profile of the Von Postbreen polythermal glacier: a) GPR interpreted profile [modified from Fig. 1a of Delf *et al*. (2022)]; b) the same GPR profile with our interpretation; the inferred radar wave velocity [m/ns] (c) and water content fraction [%] (d) [modified from Delf *et al*. (2022)]. In panels a and b, the top of the anomalous zone is marked in yellow (dashed line), the basal deposits in cyan, the glacier surface in pink (straight line); CTZ = cold/temperate-ice transition zone, WI = warm ice, CI = cold ice, AZ = anomalous zone. In panels c and d, the dashed yellow line marks the top of the AZ found with the integrated attribute analysis and described in the following paragraphs (refer to Figs. 3, 4, and 5).
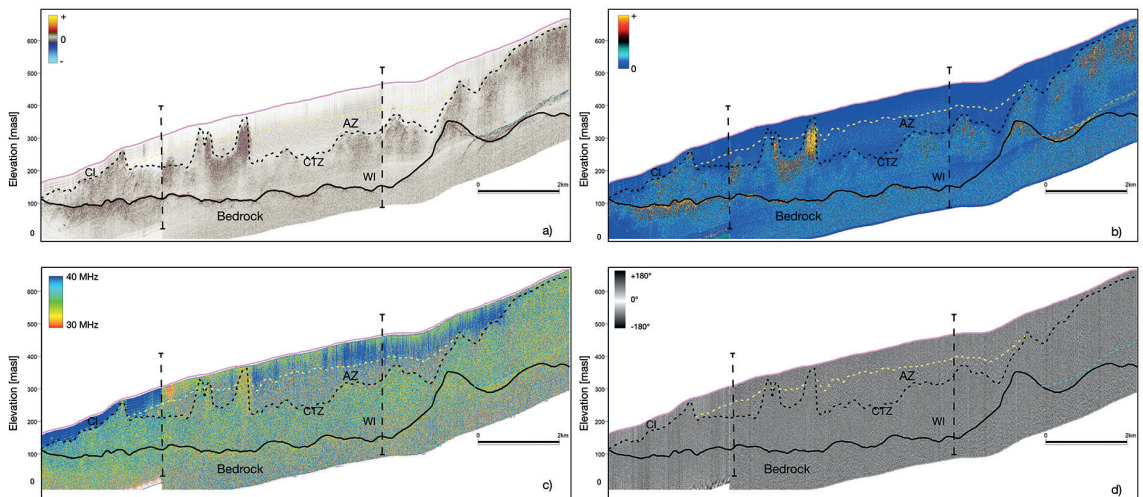

Fig. 3 - GPR attribute analysis on the GPR longitudinal profile of the Von Postbreen polythermal glacier as in Fig. 2: a) amplitude data; b) sweetness; c) dominant frequency; d) instantaneous phase. The top of the AZ is marked in yellow (dotted line), the top of the basal deposits in cyan, the glacier surface in pink (straight line); CTZ = cold/temperate-ice transition zone, WI = warm ice, CI = cold ice, AZ = anomalous zone. Vertical dashed lines mark the limits between consecutive GPR profiles.

imaged. For the sake of clarity, its top is superimposed on Figs. 2c and 2d (dashed yellow line). Interestingly, the AZ does not cross the entire section but only the central part of the glacier and some profiles crossing the central line. This peculiar and anomalous pattern is independent of data processing and is not related to data artefacts, noises, or local anomalous amplitudes, as testified by Fig. 3 in which the AZ crosses the limits (marked with vertical dashed segments) between consecutive profiles subsequently collected.

The AZ presents distinctive characteristics. It is quite different from all the other glaciological facies and is apparent as a low dominant frequency area (Fig. 3c) with intermediate sweetness values (Fig. 3b) and a peculiar phase pattern, which differs especially from the shallowest portion of the glacier (Fig. 3d).
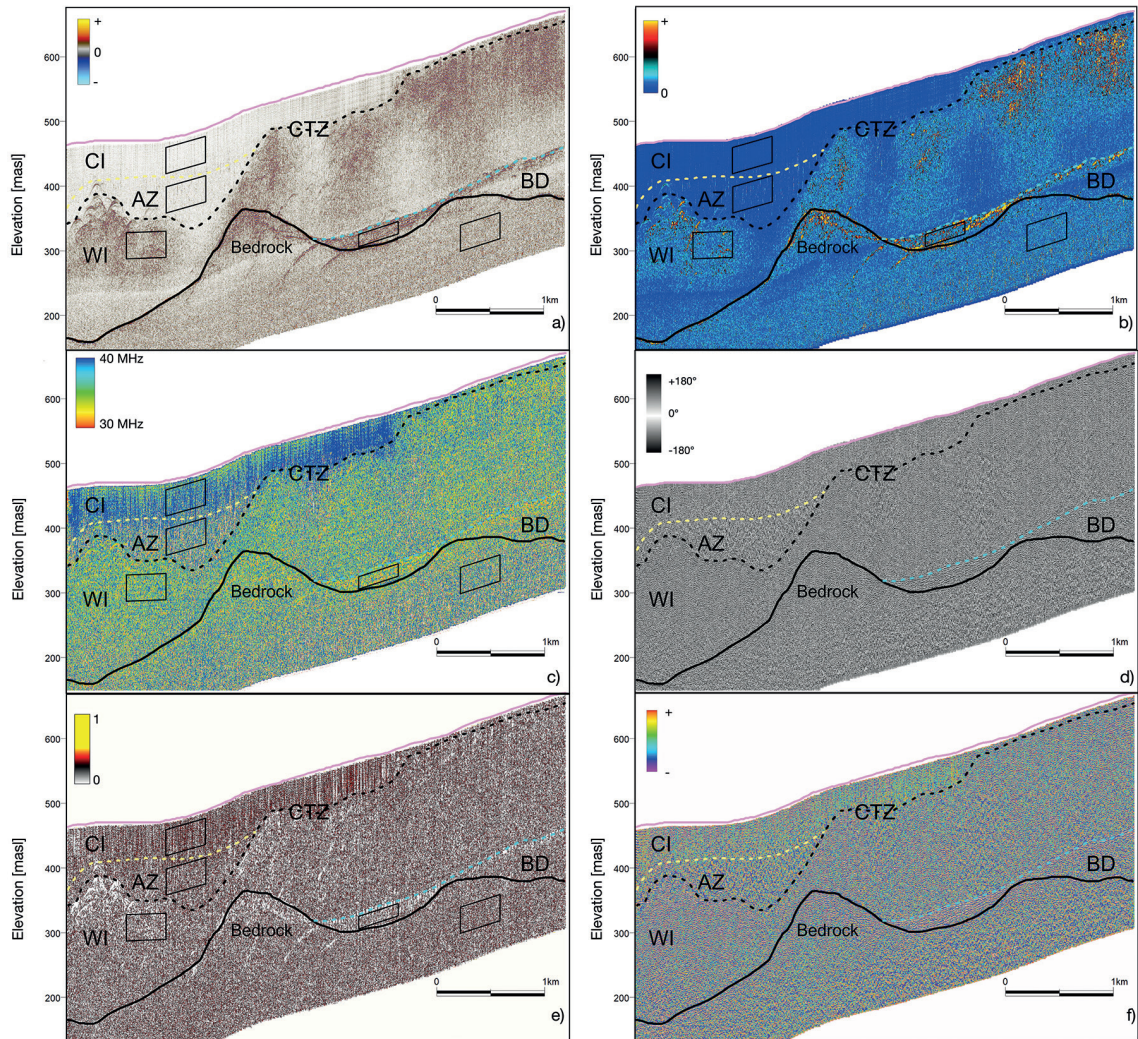

Fig. 4 - Close-up of a portion of the longitudinal GPR section of the Von Postbreen polythermal glacier where a local uplift of the bedrock is imaged: a) amplitude data; b) sweetness; c) dominant frequency; d) instantaneous phase; e) chaos; and f) entropy. The top of the AZ is marked in yellow (dotted line), the basal deposits in cyan (dotted line), the glacier surface in pink (straight line); CTZ = cold/temperate-ice transition zone, WI = warm ice, CI = cold ice, AZ = anomalous zone, BD = basal deposit. Black polygons border zones used for statistical analyses reported in Table 1.

Table 1 shows the statistical analyses performed on selected portions of GPR data (see Fig. 4 for their location), which are paradigmatic of the different interpreted zones of the glacier. In detail, the following were considered: cold ice, warm ice, AZ, basal deposit, and bedrock. Even though the standard deviation is always very high, by demonstrating a large variability of the considered attributes in all the zones, the analysis reveals a number of remarkable trends.

The AZ mean amplitude is low and similar to that of cold ice, as is the sweetness attribute. The AZ mean dominant frequency is lower than that of both cold and warm ice. While a frequency decrease is expected when passing from cold ice (shallower) to the AZ (deeper), this does not occur between the AZ and warm ice. In fact, the AZ is characterised by a low frequency shadow attributable to peculiar EM characteristics. The chaos (as well as the entropy) of the AZ is the highest of all the considered zones, as no regular patterns are present here.

Table 1 - Statistical analyses calculated on a number of GPR attributes for different EM facies (see Fig. 4 for the analysis locations).

MEAN				
	Amplitude	Dominant Frequency [MHz]	Sweetness [MHz$^{-1/2}$]	Chaos
Cold ice	6.46	38.91	1.69	0.35
AZ	9.70	35.09	2.94	0.43
Warm ice	34.97	36.91	9.42	0.28
Basal deposit	49.04	34.68	13.71	0.20
Bedrock	29.40	34.99	8.55	0.39
σ %				
	Amplitude	Dominant Frequency	Sweetness	Chaos
Cold ice	92.88	20.30	72.19	60.00
AZ	82.58	32.92	74.83	46.51
Warm ice	82.04	21.08	59.45	71.43
Basal deposit	79.71	22.90	56.75	85.00
Bedrock	79.66	30.12	58.48	51.28

If the close-up shown in Fig. 4 is taken into consideration, the anomalous pattern is very close (about 50 m) to a local uplift of the bedrock. It is apparent that the AZ is characterised by high values of chaos and entropy attributes (Figs. 4e and 4f, respectively) with a texture that is different not only from the warm ice below, but also from the shallowest cold ice. Conversely, towards the terminus of the glacier (Fig. 5) the anomaly is still present but is limited to the zones where the ice thickness exceeds by about 200 m. Here the AZ is apparent and very similar to the upper part of the glacier in terms of dominant frequency (Fig. 5c), while in terms of sweetness, it is quite similar to the shallow cold ice (Fig. 5b).

In order to check the lateral extension of the AZ, with respect to the previously analysed longitudinal profile, all GPR data available were plotted onto their actual geographic location, taking topography into account (Fig. 6). Unfortunately, there are no transversal profiles in the upper and central part of the glacier (Fig. 1) where the anomalous zone is more continuous. Instead, the transversal profiles are concentrated towards the front. However, based on the data available, the lateral transversal extension of the AZ seems to be limited to the central part of the glacier (Fig. 6). This is an interesting result, which supports the reasoning that a larger thickness of ice favours the presence of the anomaly. Moreover, local conditions are likely to play a role since the anomaly is not laterally continuous.
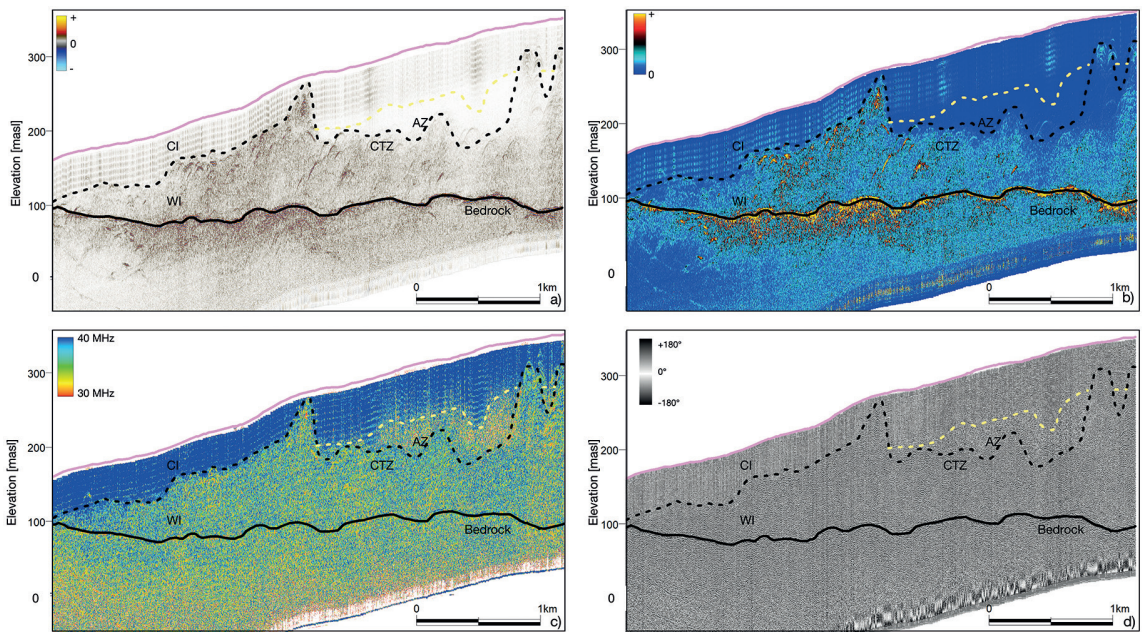
Fig. 5 - Close-up of a portion of the longitudinal GPR section of the Von Postbreen polythermal glacier where the anomalous zone is only locally present: a) amplitude data; b) sweetness attribute; c) dominant frequency attribute; d) instantaneous phase attribute. The top of the AZ is marked in yellow (dotted line), the basal deposits in cyan (dotted line), the glacier surface in pink (straight line); CTZ = cold/temperate-ice transition zone, WI = warm ice, CI = cold ice, AZ = anomalous zone.
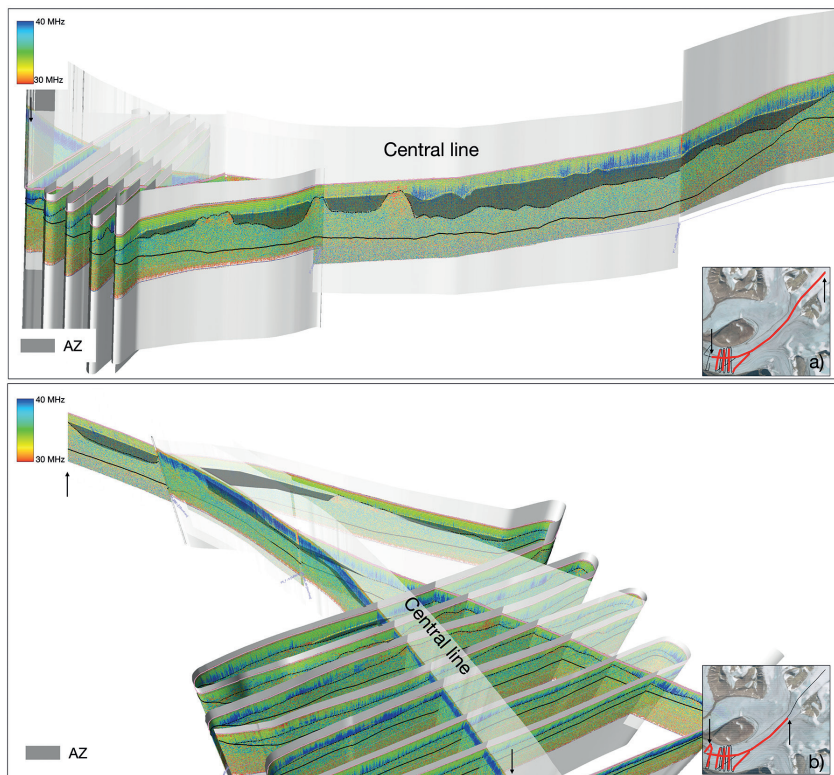

Fig. 6 - 3D view of part of the Von Postbreen polythermal glacier GPR survey: a) dominant frequency GPR attribute section, b) dominant frequency GPR attribute section. Attention should be drawn to the low-frequency anomaly (marked in transparent grey) and the lateral continuity of the AZ, also, in the transversal GPR profiles. The black line marks the glacier bottom, while the yellow dotted line marks the top of the AZ.

4. Discussion

Based on the analysis in this paper, some glaciological inferences about the AZ correlation with the ice temperature and thermal regime of the glacier can be made:

1. different thermal regimes inside the glacier are not only related to the occurrence of warm/cold ice zones and to different free water contents, but they could also be related to the existence of a capillary fringe that could extend the CTZ boundary towards the cold ice zone. This capillary fringe could be detected by the GPR in terms of an anomalous phase and frequency content, which, in turn, are related to variations of EM parameters, such as overall electrical conductivity, dielectric contrast, and attenuation (Mäzler and Wegmüller, 1987; MacGregor *et al*., 2015);

2. a local thermal effect, responsible for the formation of the AZ, could be related to the firnification and refreezing processes. This can be inferred from the fact that the anomaly occurs in the central portion of the glacier where both the maximum glacier thickness and the Equilibrium Line Altitude (ELA) lie. An effect due to the transition between the accumulation/ablation zones could, therefore, be responsible for the peculiar behaviour of the EM waves. In fact, according to Campbell *et al*. (2012) and Gusmeroli *et al*. (2013), the percolation water of the firnification process and the release of latent heat originating in the ELA zone, could affect the glacial body in terms of different amounts of water and heat. This could be visualised in the GPR data as a free-of-scattering (i.e. EM transparent) zone, as seen in the reinterpreted data herein;

3. the interaction between ice with the bedrock morphology can produce a peculiar thermal effect due to the different stress-strain rate inside the glacier. The AZ is often observed to occur downstream of a local bedrock uplift (e.g. Figs. 3c and 4) where a local temperature anomaly, due to additional heat transfer within the glacier, can be present. This effect occurs in the higher part of the glacier but not close to its terminus (Fig. 5).

To explain the nature of the anomaly in the higher part of the glacier, the third above-mentioned hypothesis is found to be the most convincing. In fact, if the work of Krabbendam (2016), in which equations are used to describe the thermal behaviour and the stress-strain relationship in a polythermal glacier for local bedrock uplift, is considered, then, some apparent similarities (Fig. 7) are encountered. Krabbendam (2016) explains that, in particular situations, the heat flux generated by the friction of the glacier on bedrock obstacles can penetrate the CTZ, and, thus, create an anomalous thermal pattern above the CTZ into the cold ice layer. Variations in the stress-strain rate and in free water volumes, moving upwards in the glacier, can equally, and further, warm the upper cold ice layer (Fig. 7).

This could describe the event that locally occurred in the Von Postbreen glacier (Fig. 4) and produced a clear frequency and phase anomaly with only a negligible effect on signal amplitude in the GPR profiles. In turn, this could be related to a negligible (and/or gradual) change of electric impedance between cold ice and the AZ, while the intrinsic attenuation of the two EM facies is different. The location of the AZ is consistent with the location of the bedrock uplift.

Concerning the lower part of the glacier, a mixing mechanism, where all the glaciological units interact together, could occur between the effects described by Krabbendam (2016) and the Von Postbreen glacier drainage system. Of note is the fact that the local CTZ uplifts towards the front (e.g. Fig. 6a), already interpreted by Krabbendam (2016) as water drainage systems, coherently exhibit very low frequency components and high sweetness values (Figs. 3c and 3b, respectively).
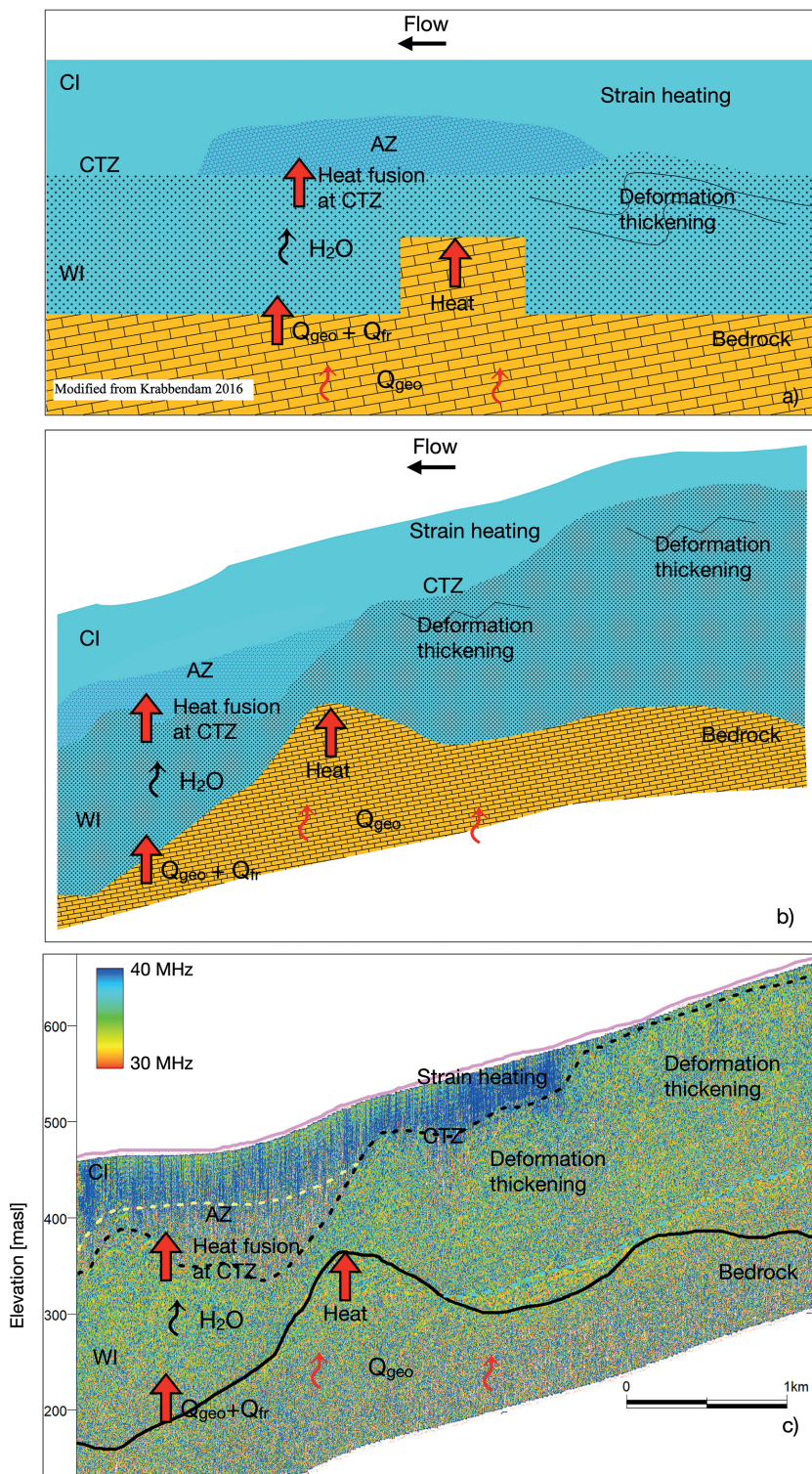
Fig. 7 - Thermal interpretation scheme of a portion of the Von Postbreen Glacier: a) scheme of the thermal growth of the temperate layer and mechanisms for heating cold ice above the CTZ (modified from Krabbendam, 2016); b) thermal interpretation scheme of a portion of the glacier (as shown in panel c); c) the dominant frequency attribute (same as in Fig. 4c).

5. Conclusions

This study demonstrates that it is possible to identify the EM facies, which occur in polythermal glaciers, in different manners. In addition, how the use of integrated GPR attributes can improve the glaciological data interpretation, by providing additional information, which otherwise cannot be extracted by considering only reflection amplitude data, has also been proven herein.

In particular, a coherent and non-ubiquitous AZ, characterised by peculiar spectral content (remarkably different from all the other GPR facies) and without any distinct amplitude behaviour, was highlighted. A similar zone can be related to local temperature variations, caused by increased heat transfer due to peculiar stress conditions. Thanks to GPR data, the extension of the AZ was mapped. The results showed that such zone is developed in the central part of the analysed glacier (more specifically, where the ice is thicker), and close to the main bedrock topographic highs. The latter condition was specifically interpreted in the light of thermal schemes taken from the literature.

Further research is needed to model heat fluxes and stress-strain patterns with a synthetic polythermal glacier model, possibly correlating these patterns to the anomalous patterns observed in the Von Postbreen polythermal glacier. The findings of this research can be applied to other glaciological GPR data sets in which the exploitation of signal attributes, and, specifically, of frequency-related attributes, provides a powerful additional geophysical interpretation tool.

REFERENCES

Bælum K. and Benn D.I.; 2011: *Thermal structure and drainage system of a small valley glacier (Tellbreen, Svalbard), investigated by ground penetrating radar*. The Cryosphere, 5, 139-149, doi: 10.5194/tc-5-139-2011.

Böniger U. and Tronicke J.; 2010: *Improving the interpretability of 3D GPR data using target-specific attributes: application to tomb detection*. J. Archaeolog. Sci., 37, 672-679, doi: 10.1016/j.jas.2010.01.013.

Böniger U. and Tronicke J.; 2012: *High-resolution GPR data analysis using extended tree-based pursuit*. J. Appl. Geophys., 78, 44-51, doi: 10.1016/j.jappgeo.2011.04.006.

Bradford J.H., Nichols J., Mikesell T.D. and Harper J.T.; 2009: *Continuous profiles of electromagnetic wave velocity and water content in glaciers: an example from Bench Glacier, Alaska, USA*. Ann. Glaciol., 50, 1-9, doi: 10.3189/172756409789097540.

Campbell S., Kreutz K., Osterberg E., Arcone S., Wake C., Introne D., Volkening K. and Winski D.; 2012: *Melt regimes, stratigraphy, flow dynamics and glaciochemistry of three glaciers in the Alaska Range*. J. Glaciol., 58, 99-109, doi: 10.3189/2012JoG10J238.

Chopra S. and Alexeev V.; 2006: *Applications of texture attribute analysis to 3D seismic data*. The Leading Edge, 25, 934-940, doi: 10.1190/1.2335155.

Chopra S. and Marfurt K.J.; 2007: *Seismic attributes for prospect identification and reservoir characterization*. Society of Exploration Geophysicists, Tulsa, OK, USA, Geophysical Developments, 11, 464 pp., ISBN 978-1-56080-141-2 (volume) - ISBN 978-0-931830-41-9 (series).

Colucci R.R., Forte E., Boccali C., Dossi M., Lanza L., Pipan M. and Guglielmin M.; 2015: *Evaluation of internal structure, volume and mass balance of glacial bodies by integrated LiDAR and GPR surveys: the case study of Canin eastern Glacieret (Julian Alps, Italy)*. Surv. Geophys., 36, 231-252, doi: 10.1007/s10712-014-9311-1.

Delf R., Bingham R.G., Curtis A., Singh S., Giannopoulos A., Schwarz B. and Borstad C.P.; 2022: *Reanalysis of polythermal glacier thermal structure using radar diffraction focusing*. J. Geophys. Res. Earth Surf., 127, e2021JF006382, 19 pp., doi: 10.1029/2021JF006382.

Forte E., Pipan M., Casabianca D., Di Cuia R. and Riva A.; 2012: *Imaging and characterization of a carbonate hydrocarbon reservoir analogue using GPR attributes*. J. Appl. Geophys., 81, 76-87, doi: 10.1016/j. jappgeo.2011.09.009.

Forte E., Santin I., Ponti S., Colucci R.R., Gutgesell P. and Guglielmin M.; 2021: *New insights in glaciers characterization by differential diagnosis integrating GPR and remote sensing techniques: a case study for the eastern Gran Zebrù glacier (central Alps)*. Remote Sens. Environ., 267, 112715, 14 pp., doi: 10.1016/j. rse.2021.112715.

Gao D.; 2011: *Latest developments in seismic texture analysis for subsurface structure, facies, and reservoir characterization: a review*. Geophys., 76, W1-W13, doi: 10.1190/1.3553479.

Geerdes I.C. and Young R.A.; 2007: *Spectral decomposition of 3D ground-penetrating radar data from an alluvial environment*. The Leading Edge, 26, 1024-1030, doi: 10.1190/1.2769560.

Gusmeroli A., Arendt A., Atwood D., Kampes B., Sanford M. and Young J.; 2013: *Variable penetration depth of interferometric synthetic aperture radar signals on Alaska glaciers: a cold surface layer hypothesis*. Ann. Glaciol., 54, 218-223, doi: 10.3189/2013AoG64A114.

Haralick R.M., Shanmugam K. and Dinstein I.; 1973: *Textural features for image classification*. IEEE Trans. Syst. Man Cybern., 3, 610-621, doi: 10.1109/TSMC.1973.4309314.

Irvine-Fynn T.L., Moorman B.J., Williams J.M. and Walter F.A.; 2006: *Seasonal changes in ground penetrating radar signature observed at a polythermal glacier, Bylot Island, Canada*. Earth Surf. Processes Landforms, 31, 892-909, doi: 10.1002/esp.1299.

King E.C., Smith A.M., Murray T. and Stuart G.W.; 2008: *Glacier-bed characteristics of midtre Lovénbreen, Svalbard, from high-resolution seismic and radar surveying.* J. Glaciol., 54, 145-156, doi: 10.3189/002214308784409099.

Krabbendam M.; 2016: *Sliding of temperate basal ice on a rough, hard bed: creep mechanisms, pressure melting, and implications for ice streaming*. The Cryosphere, 10, 1915-1932, doi: 10.5194/tc-10-1915-2016.

Lamsters K., Karušs J., Krievāns M. and Ješkins J.; 2020: *The thermal structure, subglacial topography and surface structures of the NE outlet of Eyjabakkajökull, east Iceland*. Polar Sci., 26, 100566, 45 pp., doi: 10.1016/j. polar.2020.100566.

MacGregor J.A., Li J., Paden J.D., Catania G.A., Clow G.D., Fahnestock M.A., Gogineni S.P., Grimm R.E., Morlighem M., Nandi S., Seroussi H. and Stillman D.E.; 2015: *Radar attenuation and temperature within the Greenland Ice Sheet*. J. Geophys. Res. Earth Surf., 120, 983-1008, doi: 10.1002/2014JF003418.

Mätzler C. and Wegmüller U.; 1987: *Dielectric properties of freshwater ice at microwave frequencies.* J. Phys. D. Appl. Phys., 20, 1623-1630, doi: 10.1088/0022-3727/20/12/013.

McClymont A.F., Green A.G., Streich R., Horstmeyer H., Tronicke J., Nobes D.C., Pettinga J., Campbell J. and Langridge R.; 2008: *Visualization of active faults using geometric attributes of 3D GPR data: an example from the Alpine Fault Zone, New Zealand.* Geophys., 73, B11-B23, doi: 10.1190/1.2825408.

Pettersson R., Jansson P. and Holmlund P.; 2003: *Cold surface layer thinning on Storglaciären, Sweden, observed by repeated ground penetrating radar surveys.* J. Geophys. Res., 108, 6004, 9 pp., doi: 10.1029/2003JF000024.

Randen T. and Sønneland L.; 2005: *Atlas of 3D seismic attributes*. In: Iske A. and Randen T. (eds), Mathematical Methods and Modelling in Hydrocarbon Exploration and Production, Mathematics in Industry, Springer, Berlin-Heidelberg, Germany, vol. 7, pp. 23-46, doi: 10.1007/3-540-26493-0_2.

Reinardy B.T.I., Booth A.D., Hughes A.L.C., Boston C.M., Åkesson H., Bakke J., Nesje A., Giesen R.H. and Pearce D.M.; 2019: *Pervasive cold ice within a temperate glacier - implications for glacier thermal regimes, sediment transport and foreland geomorphology*. The Cryosphere, 13, 827-843, doi: 10.5194/tc-13-827-2019.

Santin I., Colucci R.R., Zêbre M., Pavan M., Cagnati A. and Forte E.; 2019: *Recent evolution of Marmolada glacier (Dolomites, Italy) by means of ground and airborne GPR surveys*. Remote Sens. Environ., 235, 111442, 11 pp., doi: 10.1016/j. rse.2019.111442.

Sevestre H., Benn D.I., Hulton N.R.J. and Bælum K.; 2015: *Thermal structure of Svalbard glaciers and implications for thermal switch models of glacier surging*. J. Geophys. Res. Earth Surf., 120, 2220-2236, doi: 10.1002/2015JF003517.

Zhao W., Tian G., Wang B. and Lin J.; 2012: *Application of 3D GPR attribute technology in archaeological investigations*. Appl. Geophys., 9, 261-269, doi: 10.1007/s11770-012-0336-2.

Zhao W., Forte E., Colucci R.R. and Pipan M.; 2016a: *High-resolution glacier imaging and characterization by means of GPR attribute analysis.* Geophys. J. Int., 206, 1366-1374, doi: 10.1093/gji/ggw208.

Zhao W., Forte E. and Pipan M.; 2016b: *Texture attribute analysis of GPR data for archaeological prospection.* Pure Appl. Geophys., 173, 2237-2251, doi: 10.1007/s00024-016-1355-3.

Zhao W., Forte E., Fontolan G. and Pipan M.; 2018: *Advanced GPR imaging of sedimentary features: integrated attribute analysis applied to sand dunes.* Geophys. J. Int., 213, 147-156, doi: 10.1093/gji/ggx541.

Corresponding author: Pietro Gutgesell
Dipartimento di Matematica, Informatica e Geoscienze, Università degli Studi di Trieste
Via Weiss 1, 34128 Trieste, Italy
Phone: +39 040 5582271; e-mail: pietro.gutgesell@phd.units.it